NETWORKS AND HETEROGENEOUS MEDIA
©American Institute of Mathematical Sciences
Volume **8**, Number **3**, September **2013**
doi:10.3934/nhm.2013.8.663
pp. **663–684**

A DYNAMICAL TWO-DIMENSIONAL TRAFFIC MODEL IN AN ANISOTROPIC NETWORK

Tibye Saumtally

Université Paris Est, GRETTIA, Ifsttar
14-20 boulevard Newton, Cité Descartes Champs sur Marne
77447 Marne la Vallée Cedex 2, France

Jean-Patrick Lebacque and Habib Haj-Salem

Ifsttar, COSYS-GRETTIA
14-20 boulevard Newton, Cité Descartes Champs sur Marne
77447 Marne la Vallée Cedex 2, France

Abstract. The aim of this paper is to build a dynamical traffic model in a dense urban area. The main contribution of this article is to take into account the four possible directions of traffic flows with flow vectors of dimension 4 and not 2 as in fluid mechanic on a plan. Traffic flows are viewed as confrontation results between users demands and a travel supply of the network. The model gathers elements of intersection theory and two-dimensional continuum networks.

1. **Introduction.** On a single road where (x,t) denotes the couple (position,time), the LWR (Lighthill, Whitham and Richards, [10, 12]) model is a first order macroscopic model: it means that the speed v is supposed to be only a function of the density $\rho(x,t)$ of vehicles: $v(x,t) = V_e(\rho(x,t))$. In other words, this model considers that the system is permanently at an equilibrium state given by the function V_e. With the relation $q(x,t) = \rho(x,t)v(x,t)$ between the flow q, the density and the speed, this equilibrium state can also be written $q(x,t) = Q_e(\rho(x,t))$, where the equilibrium function Q_e is known as the LWR *Fundamental Diagram*. It is defined as $Q_e(\rho) = \rho V_e(\rho)$. The LWR model can be expressed by a single conservation law:

$$\partial_t \rho + \partial_x Q_e(\rho) = 0. \tag{1}$$

The function Q_e is constructed with two equilibrium functions: the equilibrium demand function Δ_e and the equilibrium supply function Σ_e. At a given point (x,t), denote x^- is the location immediately upstream of x and x^+ the location immediately downstream of x. The local demand and supply functions are defined as in [7]:

$$\Delta(x,t) = \Delta_e(\rho(x^-,t),x^-), \tag{2}$$
$$\Sigma(x,t) = \Sigma_e(\rho(x^+,t),x^+). \tag{3}$$

2010 *Mathematics Subject Classification.* Primary: 35Q99, 35Q35; Secondary: 91F99.
Key words and phrases. Traffic network, network supply, users' demand, partial differential equations, dynamical model.

The traffic flow equilibrium can be seen as the result of a demand and a supply, this equilibrium being characterized by the min-*formula*:

$$q(x,t) = \min(\Delta(x,t), \Sigma(x,t)) \tag{4}$$

It means that the resulting traffic flow is generated by the competition between users' demand which expresses users' velocity wish and link supply which expresses the users' need of security (respect of a high enough inter-vehicular distance), see Figure 1. The demand and supply functions are key concepts in traffic theory, they will be used in the two-dimensional model developed in this article (section 7).

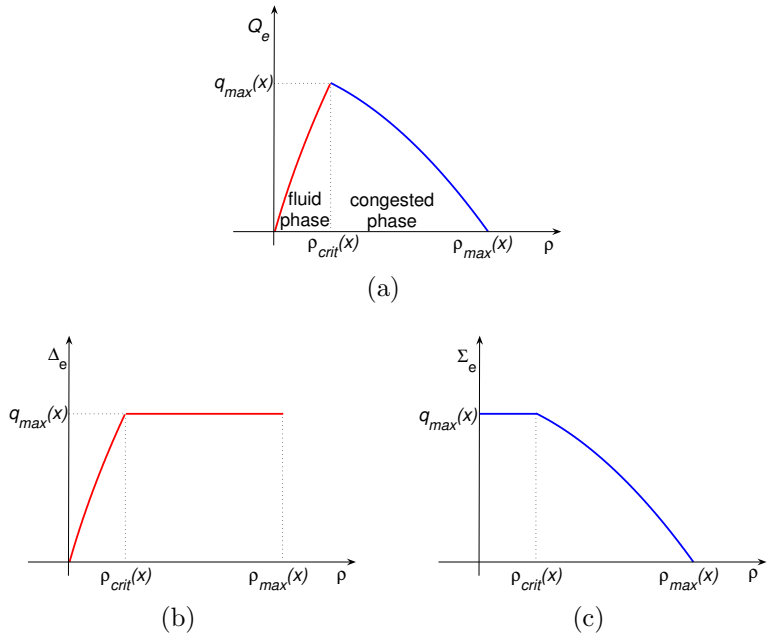

FIGURE 1. Fundamental Diagram (a), demand (b) and supply (c) functions at position x. The min-*formula* is $Q_e = \min(\Sigma_e, \Delta_e)$.

An intersection is given with I entering links numbered with $i \in \{1, \dots, I\}$, and J exiting links numbered with $j \in \{1, \dots, J\}$. All the links can have arbitrarily long length. The demand for vehicles exiting link i (towards the intersection) is δ_i. The supply for vehicles entering link j is σ_j. The problem to examine first is to determine the traffic flows denoted q_i on upstream links i and r_j on downstream links j (figure 2).

2. A brief literature review.

In this section, we will not take into account models built exclusively for merges or diverges because our goal is to build a model for large networks.

2.1. Pointwise intersections.

A pointwise model of intersection connects intersection's upstream flows q_i and downstream flows r_j. These models solve a generalized Riemann problem on the intersection. The unknowns which have to be

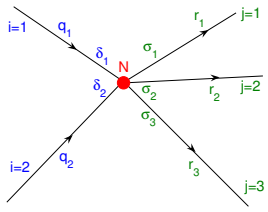

FIGURE 2. Pointwise intersection - the Riemann problem

determined are the upstream and downstream flows. The common constraints of these models are:

$$\forall i,\ 0 \leqslant q_i \leqslant \delta_i, \tag{5}$$

$$\forall j,\ 0 \leqslant r_j \leqslant \sigma_j. \tag{6}$$

2.1.1. *Holden and Risebro's model.* This model, published in [5] aims at maximize a concave function of the flows q_i and r_j under the basic constraints (5) and (6), plus a constraint called by the authors: *Rankine-Hugoniot condition for the intersections.* This last constraint expresses the conservation of vehicles that cross the intersection:

$$\sum_{i=1}^{I} q_i = \sum_{j=1}^{J} r_j. \tag{7}$$

At an intersection, users' behaviour is subjected to a *least resistance* principle. It means for instance that users who want to turn right will not turn right if the lane to their right is congested. They would choose another link (for instance, they would go straight and turn right at the next intersection). In the case of a high congested network, the *least resistance* principle seems to suggest that the destination of each user could depend on the traffic state on the network, which is not reasonable. Whether the behaviour of avoiding congested links could correspond to reality in some cases, it is far from easy to determine a realistic mathematical model of this behaviour.

The important point of this model is the maximization criterion of the normalized flows from a strictly concave function. Even if they do not give any argument to explain why it is a relevant feature from a physical point of view, this criterion allows a unique solution to the generalized Riemann problem. We will see in section 2.1.4 that this idea has a good physical interpretation for traffic flow.

2.1.2. *Turning movements coefficients.* The coefficients $(\gamma_{ij})_{ij}$ are the intersection turning movement coefficients. For any couple (i, j), γ_{ij} is the proportion of users of link i bound for link j. We have the relations:

$$0 \leqslant \gamma_{ij} \leqslant 1, \tag{8}$$

$$\forall i,\ \sum_{j=1}^{J} \gamma_{ij} = 1. \tag{9}$$

At the intersection location, the vehicles conservation is expressed by the constraint:

$$\forall j,\ r_j = \sum_{i=1}^{I} \gamma_{ij} q_i. \tag{10}$$

Constraint (10) implies the *Rankine-Hugoniot condition* (7) for intersections. It has to be kept in mind that the intersection turning movement coefficients are a local issue: while giving these coefficients at each intersection of the network, the model point of view is not focused on origin-destination travels. The idea of these intersection turning movement coefficients could be explained in the following way: at an intersection, someone is looking at the traffic flows, he does not know anything about the origins and the destinations of the vehicles he observes, but he can count vehicles and notice the vehicles turning movements, then he can calculate these coefficients.

In general, intersection turning movements coefficients are set once and for all, but they should vary with traffic conditions, what is the delicate point in the Holden and Risebro's model. Nevertheless, the possibility of making them vary is very tough because a modification on the turning movement coefficients on a given intersection has to modify the turning movements coefficients of the nearest intersections and so on. Find a criterion for such modifications seems to be very difficult: no survey has been giving such a criterion till now.

2.1.3. *Coclite and Piccoli's model.* This model has been published in 2002 in [2] and updated in 2005 in [3]. It aims at maximize the sum of the entering flows of the intersection (or equivalently with the *Rankine-Hugoniot condition* (7), the sum of the exiting flows). To obtain a unique solution, the authors impose to the intersection turning movement coefficients the relations:

$$0 < \gamma_{ij} < 1, \tag{11}$$

$$\forall (i, i'),\ i \neq i' \Rightarrow \gamma_{ij} \neq \gamma_{i'j}. \tag{12}$$

The criterion to maximize, the sum of the flows, seems to be relevant in case of an intersection regulated by traffic lights. However, in case of an intersection without any regulation, this criterion does not fit with the user's equilibrium principle of Wardrop [14]. As a matter of fact, each user will try to maximize his own speed, trying to cross the intersection as fast as possible. The maximization of the sum of flows would fit better to a social optimum.

Moreover, condition (12), though it gives a unique solution to the problem, does not have any physical sense.

2.1.4. *Lebacque's model.* Let us denote $q = (q_i)_{i=1\dots I}$ and $r = (r_j)_{j=1\dots J}$. The Lebacque's optimization model for intersections ([8, 9]) is:

$$\max_{q,r} \left\{ \sum_{i=1}^{I} \Phi_i(q_i) + \sum_{j=1}^{J} \Psi_j(r_j) \right\} \tag{13}$$

$$\text{under constraints} \begin{cases} \forall i \in \{1, \dots, I\}, & 0 \leqslant q_i \leqslant \delta_i, \\ \forall j \in \{1, \dots, J\}, & 0 \leqslant r_j \leqslant \sigma_j, \\ \forall j \in \{1, \dots, J\}, & r_j - \sum_{i=1}^{I} \gamma_{ij} q_i = 0. \end{cases}$$

The functions Φ_i and Ψ_j have to be specified.

If all the functions Φ_i and Ψ_j are equal to the *Identity function*, the criterion is the sum of the intersection entering and exiting flows. However, this criterion does not reflect the real traffic physic at an intersection without regulation and does not give a unique solution for the constraint system of (13).

The Lebacque's model supposes that functions Φ_i and Ψ_j are increasing and strictly concave functions. This property expresses what happens at the intersection: the impact of users competition for the resource represented by the space allowed by the intersection. More precisely, for instance on an entering link i with capacity k_i, the conditions should be:

$$\begin{cases} \Phi_i(0) = 0, \\ \Phi_i \text{ is strictly concave}, \\ \Phi_i \text{ is increasing on } [0, k_i], \\ \Phi_i \text{ is differentiable}. \end{cases} \tag{14}$$

Conditions (14) imply that:

$$\begin{cases} \Phi_i \text{ is strictly increasing on } [0, k_i], \\ \Phi_i'(0) > 0. \end{cases} \tag{15}$$

Obviously, the same conditions hold for Ψ_j. The functions Φ_i and Ψ_j can be interpreted as intersection's attributes, as we are going to explain it.

Let us denote:

$$\begin{cases} a = (a_i)_i, & a_i \geqslant 0, & \forall i \in \{1 \dots I\}, \\ b = (b_i)_i, & b_i \geqslant 0, & \forall i \in \{1 \dots I\}, \\ c = (c_j)_j, & c_j \geqslant 0, & \forall j \in \{1 \dots J\}, \\ d = (d_j)_j, & d_j \geqslant 0, & \forall j \in \{1 \dots J\}, \\ e = (e_j)_j, & e_j \in \mathbb{R}, & \forall j \in \{1 \dots J\}. \end{cases}$$

We build the Lagrangian:

$$\begin{aligned} \mathscr{L}(q, r, a, b, c, d, e) = & \\ & - \sum_{i=1}^{I} \Phi_i(q_i) - \sum_{j=1}^{J} \Psi_j(r_j) \\ & - \sum_{i=1}^{I} a_i q_i + \sum_{i=1}^{I} b_i (q_i - \delta_i) - \sum_{j=1}^{J} c_j r_j + \sum_{j=1}^{J} d_j (r_j - \sigma_j) \\ & + \sum_{j=1}^{J} e_j \Big(r_j - \sum_{i=1}^{I} \gamma_{ij} q_i \Big). \end{aligned} \tag{16}$$

The Kuhn-Tucker coefficients (a_i), (b_i), (c_j), (d_j), (e_j) verify the relations:

$$\begin{cases} \frac{\partial \mathscr{L}}{\partial q_i}(q, r, a, b, c, d, e) = 0, \\ \frac{\partial \mathscr{L}}{\partial r_j}(q, r, a, b, c, d, e) = 0. \end{cases}$$

or equivalently:

$$\begin{cases} \Phi_i'(q_i) = -a_i + b_i - \sum_{j=1}^{J} e_j \gamma_{ij}, \\ \Psi_j'(r_j) = -c_j + d_j + e_j. \end{cases} \tag{17}$$

The relations (17) are going to give us the interpretations of functions Φ_i and Ψ_j with respect to the intersection supply and the intersection demand. For instance, for functions Φ_i and flows q_i:

- ⋆ If $0 < q_i < \delta_i$, then $a_i = 0$ and $b_j = 0$, $\Phi_i'(q_i) = -\sum_{j=1}^{J} e_j\gamma_{ij}$.
  As Φ_i' is strictly decreasing: $q_i = \Phi_i'^{-1}(-\sum_{j=1}^{J} e_j\gamma_{ij})$.
- ⋆ If $0 = q_i$, then $b_i = 0$ (and $a_i \geqslant 0$), $\Phi_i'(q_i) = -a_i - \sum_{j=1}^{J} e_j\gamma_{ij}$.
  Then $\Phi_i'(q_i) \leqslant -\sum_{j=1}^{J} e_j\gamma_{ij}$ and as Φ_i' is strictly decreasing:
  $q_i \geqslant \Phi_i'^{-1}(-\sum_{j=1}^{J} e_j\gamma_{ij})$.
- ⋆ If $q_i = \delta_i$, then $a_i = 0$ (and $b_j \geqslant 0$), $\Phi_i'(q_i) = b_i - \sum_{j=1}^{J} e_j\gamma_{ij}$.
  Then $\Phi_i'(q_i) \geqslant -\sum_{j=1}^{J} e_j\gamma_{ij}$ and as Φ_i' is strictly decreasing:
  $q_i \leqslant \Phi_i'^{-1}(-\sum_{j=1}^{J} e_j\gamma_{ij})$.

Let us denote $\Pi_{[a,b]}(x)$ the projection of an element x on the line segment $[a, b]$. The projection function $\Pi_{[a,b]}$ is defined as:

$$\begin{array}{rccc} \Pi_{[a,b]}: & \mathbb{R} & \longrightarrow & \mathbb{R} \\ & x & \longmapsto & \begin{cases} a & \text{if } x < a \\ x & \text{if } x \in [a,b] \\ b & \text{if } x > b \end{cases} \end{array}$$

The previous study leads to:

$$q_i = \Pi_{[0,\delta_i]}\big(\Phi_i'^{-1}(-\sum_{j=1}^{J} e_j\gamma_{ij})\big). \tag{18}$$

If we notice that the projection of an element x on line segment $[a, b]$ can be written $\Pi_{[a,b]}(x) = \min(\max(a, x), b)$, then (18) can be written as:

$$q_i = \min\left(\max\left(0, \Phi_i'^{-1}(-\sum_{j=1}^{J} e_j\gamma_{ij})\right), \delta_i\right). \tag{19}$$

The quantity $\max\left(0, \Phi_i'^{-1}(-\sum_{j=1}^{J} e_j\gamma_{ij})\right)$ can be interpreted as an implicit intersection supply for the upstream link i, given that δ_i is the demand on the link i entering in the intersection.

The same type of study leads to

$$r_j = \Pi_{[0,\sigma_j]}\big(\Psi_j'^{-1}(e_j)\big). \tag{20}$$

The quantity $\max\left(0, \Psi_j'^{-1}(e_j)\right)$ can be interpreted as an implicit intersection demand for the downstream link j, given that σ_i is the supply on the link j exiting the intersection.

2.2. **Internal state intersection model.** A simple intersection model is developed in [8, 9]. It can be explained as follows. The intersection is not considered anymore as a point but as a "box" (figure 3.a). It means that the intersection can contain vehicles. Hence, if there are N vehicles in the intersection, waiting for entering their exit link, the intersection state is characterized by a supply $\Sigma(N)$ and a demand $\Delta(N)$. These supply and demand functions Σ and Δ are supposed to have the same shape as link supply and link demand (figure 1). The maximum number of vehicles in the intersection will be noted $N_{\max}$, the maximum flow $Q_{\max}$

through the intersection will be reached for a critical number N_{crit} of vehicles in the intersection.

If there are N vehicles in the intersection, each incoming link will have an incoming supply noted $\Sigma_i(N)$. From empirical data in [8], $\Sigma_i(N)$ is given by a linear split of $\Sigma(N)$: $\Sigma_i(N) = \beta_i \Sigma(N)$. The coefficients β_i have a physical sense which can be difficult to understand. They represent the fraction of accessible lanes to users from link i. In case there are more entering lanes than exiting lanes, it is possible that $\sum_{i=1}^{I} \beta_i > 1$. We are going to explain how this could happen with figure 3.b: users coming from link 1 find accessible the exit link, and users coming from link 2 too. Thus, $\Sigma_1(N) = \Sigma(N)$, $(\beta_1 = 1)$ and $\Sigma_2(N) = \Sigma(N)$, $(\beta_2 = 1)$. What would happen if we imposed for instance $\beta_1 = \frac{1}{2}$ and $\beta_2 = \frac{1}{2}$? The intersection would fill more slowly than in the previous case.

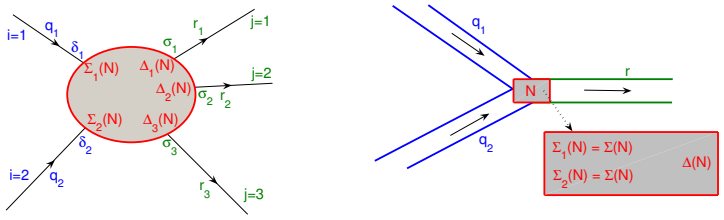

(a) (b)

FIGURE 3. Pointwise intersection - Generalized Riemann problem (a). Intersection with $\beta_1 = 1$ and $\beta_2 = 1$ (b).

If N_j denotes the number of vehicles in the intersection bound for link j (obviously, $\sum_j N_j = N$), the partial demand Δ_j for downstream link j is assumed to be proportional to N_j: $\Delta_j = \frac{N_j}{N}\Delta(N)$.

The conservation of vehicles in the intersection is given by the formula: $\frac{\mathrm{d}}{\mathrm{d}t}N_j = \sum_i \gamma_{ij} q_i - r_j$, with the usual formulas for flows: $q_i = \min(\delta_i, \Sigma_i)$ and $r_j = \min(\Delta_j, \sigma_j)$.

The important point is that both Lebacque's models (sections 2.1.4 and 2.2) satisfy the *Invariance Principle* ([8, 9]). The *Invariance Principle* can be stated as follows:

- ⋆ If $q_i < \delta_i$, then q_i is equal to the supply. Hence, the flow q_i is unchanged if the demand δ_i is increased up to $Q_{i,\max}$.
- ⋆ If $r_j < \sigma_j$, then r_j is equal to the demand. Hence, the flow r_j is unchanged if the supply σ_j is increased up to $Q_{j,\max}$.

In case of equilibrium ($\frac{\mathrm{d}}{\mathrm{d}t}N_j = 0$), it is proved in [9] and [8] that internal state model and pointwise optimization model are equivalent for merges and diverges.

3. **Experiences on a large orthotropic network.** We aim at finding a two-dimensional behaviour law. Can such a law be found in the center of a large orthotropic network with $K \times L$ intersections (figure 4)? On each intersection (k, l), we know the turning node movements γ_{ij}^{kl} which are supposed to be constant.

The number γ_{ij}^{kl} represents the proportion of vehicles that go from link i to link j at node (k,l). For sake of simplicity, each link has a distance of 1, hence, between two intersections, the distance is 2. It is important to underline that we do not take into account an origin-destination point of view, we are only interested in vehicles circulation on the network. We are looking for a static traffic equilibrium with constant supplies and demands.

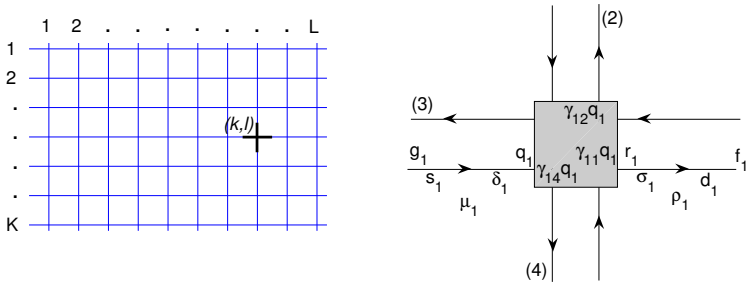

(a) (b)

FIGURE 4. Orthotropic network with K lines and L columns (a). Zoom on a network element (b): on each node entering link, the density is μ, there is a supply s and a flow g at its beginning, a demand δ and a flow q at the intersection entry; the split of the entering flows is given by γ coefficients; on each node exiting link the density is ρ, there is a supply σ and a flow r at its beginning (after the intersection), a demand d and a flow f at the link exit.

We are going to test the Lebacque's intersection models on this network using algorithm 1.

3.1. **Common data.** The turning movement coefficients are the same at each intersection. This hypothesis can be seen as quite artificial, but in a big homogenous network, turning movement coeficients should be nearly the same on nearby intersections. The matrix which represents these coefficients in our test network is:

$$(\gamma_{ij})_{ij} = \begin{pmatrix} 0.4686 & 0.2236 & 0 & 0.3078 \\ 0.0405 & 0.469 & 0.4905 & 0 \\ 0 & 0.3109 & 0.2904 & 0.3987 \\ 0.3512 & 0 & 0.4097 & 0.2391 \end{pmatrix}$$

Each link is one kilometer long and the Fundamental Diagram on each link is as in figure 5: the capacity is of 50 vehicles per minute, the critical density is of 60 vehicles per kilometer, the fluid regime velocity is of 50 kilometers per hour.

The demands at the entry of border links are set equal to 25 vehicles per minute and the supplies at the exits of the border links are set equal to 50 vehicles per minute.

3.2. **Test with pointwise optimization model.** Functions Φ_i are set equal for any $i \in \{1,2,3,4\}$, functions Ψ_j are set equal for any $j \in \{1,2,3,4\}$. They are defined as:

$$\begin{array}{rccc} \Phi: & \mathbb{R} & \longrightarrow & \mathbb{R} \\ & q & \longmapsto & -q^2 + 140q \end{array} \qquad \begin{array}{rccc} \Psi: & \mathbb{R} & \longrightarrow & \mathbb{R} \\ & r & \longmapsto & -r^2 + 160r \end{array}$$

Algorithm 1 Large orthotropic discrete network algorithm

Input: ⋆ K lines and L columns,
⋆ turning movement coefficients,
⋆ pointwise model case: definition of functions Φ_i and Ψ_j,
⋆ internal state model case: definition of intersection demand and supply functions,
⋆ Fundamental Diagrams on links,
⋆ border conditions: supplies s_i^{kl} and demands d_i^{kl} at the network entries and exits,
⋆ ending time T.
(For sake of simplicity, in the sequel, we omit the indices i, k, l)

empty network initial conditions (at $t = 0$): ρ^0 and μ^0 are null on each link
for $t = 0$ to T **do**
  Calculate s^t, δ^t, σ^t and d^t with the Supply and Demand splits of the Fundamental Diagram
  Calculate g^t, q^t, r^t and f^t with the min-*formula*
  Calculate $\rho^{t+1} = \rho^t + r^t - f^t$, $\mu^{t+1} = \mu^t + g^t - q^t$
end for
Output: ⋆ the flows g^T, q^T, r^T and f^T,
⋆ the densities μ^T and ρ^T,
⋆ the supplies and demands s^T, δ^T, σ^T and d^T.

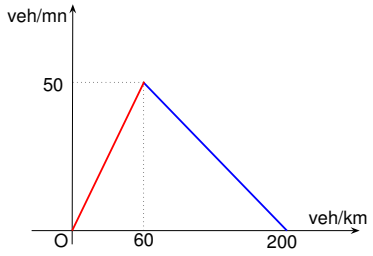

FIGURE 5. Fundamental Diagram at each point of each link. Each link is of length 1km. At each point, the capacity is of 50 veh.mn^{-1}, the critical density is of 60 veh.km^{-1}, the fluid phase velocity is of 50 km.h^{-1}.

They verify conditions (14). In particular, critical values for Φ (70 veh.mn^{-1}) and for Ψ (80 veh.mn^{-1}) are superior to the link capacities (50 veh.mn^{-1}), as required.

With the graphs of figure 6, we can hypothesize a behaviour law at the center intersection of a network composed with the same turning movement matrix γ at each intersection: the entering flow vector (q_1, q_2, q_3, q_4) is an eigenvector of matrix ${}^t\gamma$ associated to the eigenvalue 1, hence the exiting flow vector (r_1, r_2, r_3, r_4) is equal to (q_1, q_2, q_3, q_4). This behaviour law can be noticed when the demands at the border are not to high: in case of high demand levels on the border, the network will reach bit-by-bit the completely blocked equilibrium state. We are now going to test if this empirical behaviour law still works in a network where intersections are treated with an internal state model.

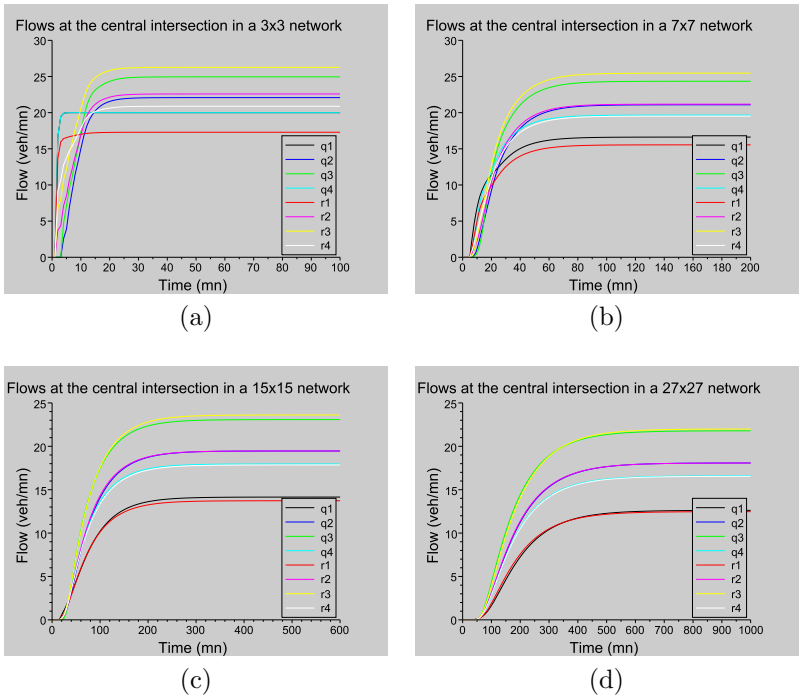

FIGURE 6. Pointwise optimization model - Traffic flows at the adjacent links of the central intersection in a 3×3 intersections network (a) and a 7×7 intersections network (b). When road traffic is fluid on the network, the equilibrium state is reached for eigenvectors of ${}^t\gamma$ associated with the eigenvalue 1. The same tests in a 15×15 intersections network (c) and a 27×27 intersections network (d) give that the equilibrium state flows and even the loading of the central intersection (transitional phase at the beginning) are made up of such eigenvectors.

3.3. **Test with internal state model.** The internal state model gives a location for vehicle stocking. According to different traffic patterns, this should allow regularizing effects when demand is low, and oscillations as demand increases. Hence, the previous behaviour law should not be so evident.

Each node characteristic supply and demand functions are defined as in figure 7. The intersection is modelled with a location which surrounds the real intersection over more or less 75 meters in each direction.

The tests should be cautious because of the model sensitivity. On figure 8, one can see that even with a quite low demand, an equilibrium state cannot be reached on the central node of a 7×7 intersections network. A general behaviour law should be obtained with lower demands on the border.

On figure 9, equilibrium states are reached at the central intersection of three networks of different sizes, with weak demands on the border. The obtained behaviour law is the same than the pointwise model behaviour law at equilibrium.

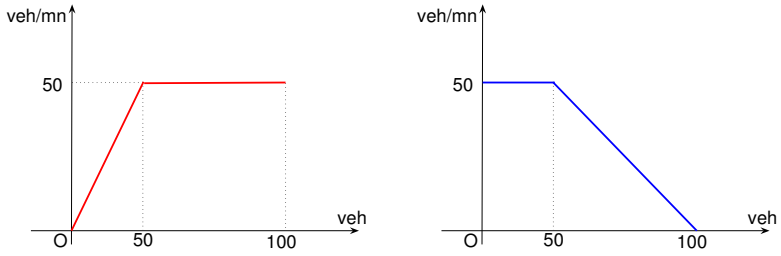

(a) (b)

FIGURE 7. Internal state model - Demand (a) and supply (b) functions for each intersection of the network. The intersection itself is provided with a demand and a supply function with same shapes as demand and supply functions for links.

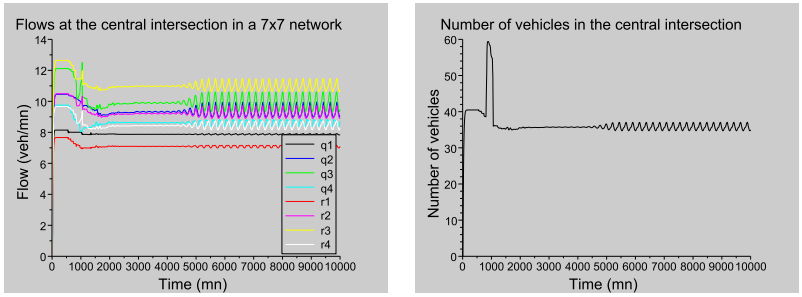

(a) (b)

FIGURE 8. Internal state model - A 7×7 intersections network: the flows at the central intersection (a) and the number of vehicles in the central intersection (b) are oscillating. The loading demand (12 veh.mn^{-1}), is quite low for links, but it is sufficient to disturb the intersections traffic state.

Nevertheless, it is more instable as far as the *Rankine-Hugoniot condition* (7) is replaced by $\frac{\mathrm{d}N}{\mathrm{d}t}(t) = \sum_{i=1}^{4} q_i(t) - \sum_{j=1}^{4} r_j(t)$.

4. **What could be improved with these models?** A general behaviour law has been found at the center of a network provided with intersections with same turning movement coefficients: the equilibrium state is given by an eigenvector of the transpose of turning movement matrix associated to the eigenvalue 1.

It is proved in [9] that the pointwise and the internal state models are equivalent for a merge and a diverge. It is shown that the merge model is compatible to experimental data. Nevertheless, many questions hold to understand better these models and compare them. For instance, if one defines the coordinates of the *critical demand vectors* as the demands on the border that break the equilibrium state at the central intersection, how to characterize these *critical demand vectors*? This would define critical regimes for intersections.

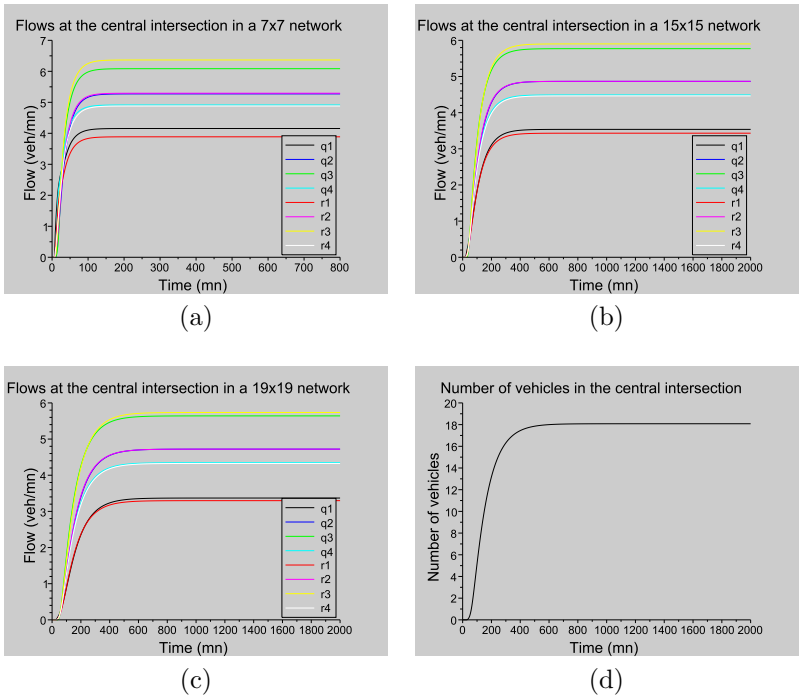

FIGURE 9. Internal state model - Traffic flows at the central intersection on 7×7 (a), 15×15 (b) and 19×19 (c) intersections networks, with low demands on the border (6 veh.mn^{-1}). For each travel direction, the equilibrium state is reached for an entering flow equal to the exiting flow. On (d), the evolution of the number of vehicles in the central intersection of the 19×19 intersections network is represented.

From now, we develop the traffic local conservation equations in a continuous anisotropic network. We target towards a dynamical equation that would take crossing traffic flows into account. To this end, we will use previous results.

5. **Anisotropic network.**

5.1. **Urban area.**

Let us denote $\mathfrak{A}$ a dense urban area with an anisotropic network. The network is considered as a continuum. It means that all the network roads are aggregated so that vehicles behave like a two-dimensional fluid, as if the area was observed from a long distance (e.g. [13, 16, 15, 11]). Hence, the detailed geometric structure is lost. Nevertheless, it doesn't mean that at a network point, vehicles can follow an arbitrary direction. In the sequel, we will suppose four possible travel directions at any inside point of the area (except on the border where only two or three directions are possible).

The area $\mathfrak{A}$ is viewed as a subset of the $\mathbb{R}^2$ Euclidean space. The anisotropic network is defined by the two angles θ_1 and θ_2 (denote $\theta = \theta_2 - \theta_1$), its local (or "natural") basis is (u_1, u_2) (figure 10.a). In the sequel, we define an arbitrary point

O chosen as the origin and we will exclusively work in the local basis (u_1, u_2). It means that a point P of the area has generical coordinates (a, b) in (O, u_1, u_2) if and only if $\overrightarrow{OP} = au_1 + bu_2$, and we will simply denote it $P(a, b)$.

Let us define $u_3 = -u_1$ and $u_4 = -u_2$. The four vectors u_1, u_2, u_3 and u_4 represent the four privileged directions of travelling in the anisotropic network (figure 12). We will simply denote these directions i instead of u_i.

5.2. **Lane density.** The density of lanes to direction i at point $P(a, b)$ is $\lambda_i(a, b)$ expressed in lanes per length unit. To obtain it, one has to count the number of lanes to direction i that intercept a line segment of length 1, orthogonal to direction i and centred on P (figure 11.b). We will suppose that $\lambda_1 = \lambda_3$ and $\lambda_2 = \lambda_4$. This means that at each point, two opposite directions are always side by side. The density functions λ_i are strictly positive. As far as the considered area is dense, and to avoid mathematical instabilities, we will suppose that density functions verify the condition:

$$\exists\, l_i > 0 / \forall P(a, b) \in \mathfrak{A},\ \lambda_i(a, b) > l_i. \tag{21}$$

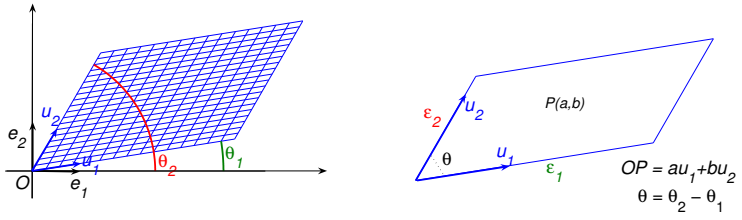

(a) (b)

FIGURE 10. Anisotropic network with orthonormal basis (e_1, e_2) and its local basis (u_1, u_2) (a). Zooming on an elementary cell (b).

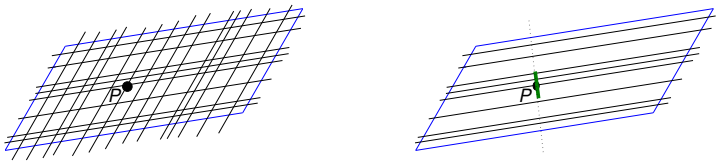

(a) (b)

FIGURE 11. Lanes on an elementary cell (a). How to calculate the density of lanes to a prescribed direction at P? (b)

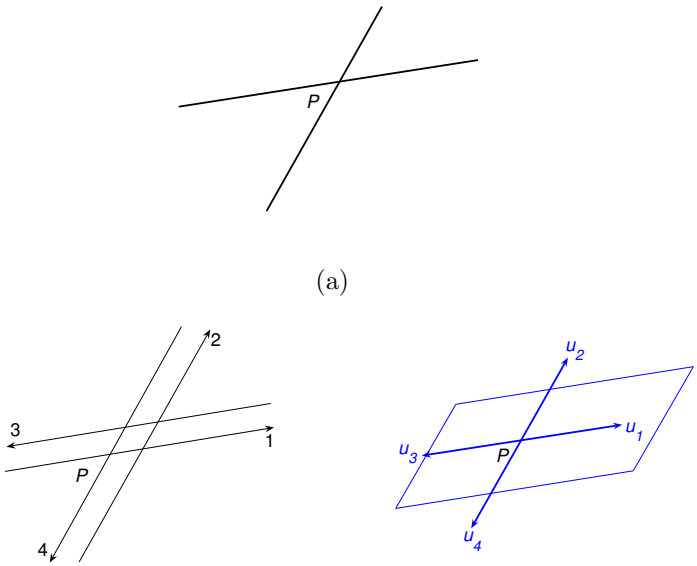

FIGURE 12. Four symbolized lanes at point P (a). The four directions at point P (b) symbolized by four vectors (c).

5.3. **Flow functions.** Functions $(q_i)_i$ represent the flow functions to direction i. At point $P(a,b)$, $q_i(a,b)$ is equal to the traffic flow on the lane to direction i. As a consequence, the functions $(f_i)_i$ defined as $f_i = \lambda_i q_i$ represent the flow functions per unit length to direction i. (At point $P(a,b)$, the quantity $f_i(a,b)$ is equal to the traffic flow per unit length to direction i.)

5.4. **Turning movement rate functions.** The functions $(\gamma_{ij})_{(i,j)\in\{1,2,3,4\}^2}$ represent the turning movement rates: at point $P(a,b)$, for all $(i,j) \in \{1,2,3,4\}^2$, the number $\gamma_{ij}(a,b)$ is the fraction of turning movements for traffic flow coming from direction i, reaching point P and then going to direction j. (We suppose there are no U-turn: if $(i,j) \in \{(1,3),(3,1),(2,4),(4,2)\}$ then $\gamma_{ij} = 0$.)

As $\gamma_{ij}(a,b)$ is a fraction, there are two obvious properties:

$$0 \leqslant \gamma_{ij}(a,b) \leqslant 1, \tag{22}$$

$$\forall i,\ \sum_{j=1}^{4} \gamma_{ij}(a,b) = 1. \tag{23}$$

In other words, property (23) expresses that the $\mathcal{M}_4(\mathbb{R})$ matrix $\gamma(a,b) = (\gamma_{ij}(a,b))_{i,j}$ is a stochastic matrix (section 10).

We will suppose a third property. It is the behaviour empirical law obtained in section 3. At each point of the area:

$$\forall j,\ q_j(a,b) = \sum_{i=1}^{4} \gamma_{ij}(a,b) q_i(a,b). \tag{24}$$

From a physical point of view, property (24) can be seen as the local conservation of vehicles at each point of the area. It means that $(q_i(a,b))_i$, which is a vector with all its coordinates positive, is an eigenvector of ${}^t\gamma(a,b)$ associated to the eigenvalue 1. Let us point out it is mathematically possible from the lemma of section 10.

6. **Conservation equation in traffic cells.** We consider a cell c of the area. The lengths of the two sides of an elementary cell (which is a parallelogram) are ϵ_1 and ϵ_2 (figure 10.b). For all $i \in \{1,2,3,4\}$, let us denote $N_i(t)$ the number of vehicles of cell c which are travelling to direction i at time t. How does vary N_i in cell c? Each direction i carries a flow q_i on each lane with density λ_i. The number N_i can vary with internal exchanges of cell c, and external exchanges with cell c.

6.1. **Internal exchanges.** What happens on direction i in cell c? At each point of coordinates (a,b), a flow $\sum_{j\neq i}\gamma_{ij}(a,b)q_i(a,b)$ exits from direction i and a flow $\sum_{j\neq i}\gamma_{ji}(a,b)q_j(a,b)$ enters with direction i. Hence, using relation (24) of vehicles conservation, the balance is:

$$\begin{aligned}
&\sum_{j\neq i}\gamma_{ji}(a,b)q_j(a,b) - \sum_{j\neq i}\gamma_{ij}(a,b)q_i(a,b)\\
&\quad= \sum_{j\neq i}\gamma_{ji}(a,b)q_j(a,b) + \gamma_{ii}(a,b)q_i(a,b) - \gamma_{ii}(a,b)q_i(a,b) - \sum_{j\neq i}\gamma_{ij}(a,b)q_i(a,b)\\
&\quad= \sum_{j}\gamma_{ji}(a,b)q_j(a,b) - \sum_{j}\gamma_{ij}(a,b)q_i(a,b)\\
&\quad= q_i(a,b) - q_i(a,b)\\
&\quad= 0. \qquad (25)
\end{aligned}$$

So the internal balance is null.

6.2. **Exchange balance in a cell.** From now, (a,b) will designate the center of cell c. For sake of simplicity, let us study the case $i=1$ (figure 13), the others are the same.

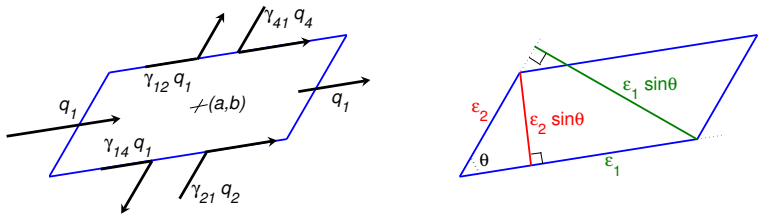

(a) (b)

FIGURE 13. Entries and exits of vehicles to direction 1 in cell c (a). Characteristic lengths (b).

$$
\begin{aligned}
&N_1(t+\Delta t) - N_1(t) = \\
&\quad q_1(a-\frac{\epsilon_1}{2},b,t)\lambda_1(a-\frac{\epsilon_1}{2},b)\epsilon_2\sin\theta\Delta t \\
&\quad - q_1(a+\frac{\epsilon_1}{2},b,t)\lambda_1(a+\frac{\epsilon_1}{2},b)\epsilon_2\sin\theta\Delta t \\
&\quad + \gamma_{21}(a,b-\frac{\epsilon_2}{2})q_2(a,b-\frac{\epsilon_2}{2},t)\lambda_2(a,b-\frac{\epsilon_2}{2})\epsilon_1\sin\theta\Delta t \\
&\quad - \gamma_{14}(a,b-\frac{\epsilon_2}{2})q_1(a,b-\frac{\epsilon_2}{2},t)\lambda_2(a,b-\frac{\epsilon_2}{2})\epsilon_1\sin\theta\Delta t \\
&\quad + \gamma_{41}(a,b+\frac{\epsilon_2}{2})q_4(a,b+\frac{\epsilon_2}{2},t)\lambda_2(a,b+\frac{\epsilon_2}{2})\epsilon_1\sin\theta\Delta t \\
&\quad - \gamma_{12}(a,b+\frac{\epsilon_2}{2})q_1(a,b+\frac{\epsilon_2}{2},t)\lambda_2(a,b+\frac{\epsilon_2}{2})\epsilon_1\sin\theta\Delta t. \qquad (26)
\end{aligned}
$$

To lighten the equation, we omit the argument (a,b,t):

$$
\begin{aligned}
&\frac{N_1(t+\Delta t) - N_1(t)}{\sin\theta\Delta t} = \\
&\quad \epsilon_2 q_1\lambda_1 - \frac{\epsilon_1\epsilon_2}{2}\partial_x q_1\lambda_1 - \epsilon_2 q_1\lambda_1 - \frac{\epsilon_1\epsilon_2}{2}\partial_x q_1\lambda_1 \\
&\quad + \epsilon_1\gamma_{21}q_2\lambda_2 - \frac{\epsilon_1\epsilon_2}{2}\partial_y\gamma_{21}q_2\lambda_2 - \epsilon_1\gamma_{14}q_1\lambda_2 + \frac{\epsilon_1\epsilon_2}{2}\partial_y\gamma_{14}q_1\lambda_2 \\
&\quad + \epsilon_1\gamma_{41}q_4\lambda_2 + \frac{\epsilon_1\epsilon_2}{2}\partial_y\gamma_{41}q_4\lambda_2 - \epsilon_1\gamma_{12}q_1\lambda_2 - \frac{\epsilon_1\epsilon_2}{2}\partial_y\gamma_{12}q_1\lambda_2 \\
&\quad + \epsilon_1\gamma_{11}q_1\lambda_2 - \epsilon_1\gamma_{11}q_1\lambda_2. \qquad (27)
\end{aligned}
$$

With vehicles conservation equation (24), and by noticing that the area of the elementary cell is equal to $\epsilon_1\epsilon_2\sin\theta$, then $\lim_{\Delta t\to 0^+}\frac{N_1(t+\Delta t)-N_1(t)}{\epsilon_1\epsilon_2\sin\theta\Delta t} = \partial_t\rho_1$. Then, for the cell which center is (a,b), we obtain the local conservation equation for traffic flows to direction 1 at time t:

$$
\partial_t\rho_1 + \partial_x f_1 + \partial_y\Big(\frac{f_2\gamma_{21} - f_4\gamma_{41}}{2} + \frac{\lambda_2}{\lambda_1}\frac{f_1\gamma_{12} - f_1\gamma_{14}}{2}\Big) = 0. \qquad (28)
$$

By the same token, we obtain the equations for directions $2, 3$ and 4:

$$
\partial_t\rho_2 + \partial_x\Big(\frac{f_1\gamma_{12} - f_3\gamma_{32}}{2} + \frac{\lambda_1}{\lambda_2}\frac{f_2\gamma_{21} - f_2\gamma_{23}}{2}\Big) + \partial_y f_2 = 0, \qquad (29)
$$

$$
\partial_t\rho_3 + \partial_x(-f_3) + \partial_y\Big(\frac{f_2\gamma_{23} - f_4\gamma_{43}}{2} + \frac{\lambda_2}{\lambda_1}\frac{f_3\gamma_{32} - f_3\gamma_{34}}{2}\Big) = 0, \qquad (30)
$$

$$
\partial_t\rho_4 + \partial_x\Big(\frac{f_1\gamma_{14} - f_3\gamma_{34}}{2} + \frac{\lambda_1}{\lambda_2}\frac{f_4\gamma_{41} - f_4\gamma_{43}}{2}\Big) + \partial_y(-f_4) = 0. \qquad (31)
$$

If we sum the equations (28), (29), (30) and (31), we obtain a global conservation equation in the cell while writing that $\rho = \rho_1 + \rho_2 + \rho_3 + \rho_4$ and using with vehicles conservation equation (24):

$$
\begin{aligned}
&\partial_t\rho + \partial_x\left(f_1 - f_3 + \frac{1}{2}\left[1 + \frac{\lambda_1}{\lambda_2}\right]\left[\big(1-\gamma_{11}\big)f_1 - \big(1-\gamma_{33}\big)f_3\right]\right) \\
&\quad + \partial_y\left(f_2 - f_4 + \frac{1}{2}\left[1 + \frac{\lambda_2}{\lambda_1}\right]\left[\big(1-\gamma_{22}\big)f_2 - \big(1-\gamma_{44}\big)f_4\right]\right) = 0. \qquad (32)
\end{aligned}
$$

Let us write equation (32) in the particular case $\lambda_1 = \lambda_2$. It becomes:

$$\partial_t \rho + \partial_x \Big(\big(2-\gamma_{11}\big) f_1 - \big(2-\gamma_{33}\big) f_3 \Big) + \partial_y \Big(\big(2-\gamma_{22}\big) f_2 - \big(2-\gamma_{44}\big) f_4 \Big) = 0. \quad (33)$$

Let us explain why equation (33) was expected. There are 5 traffic flows that enter the elementary cell on each side. For instance, on figure (14), we add the 5 flows that enter the cell from the left side: $\gamma_{41}q_4 + \gamma_{11}q_1 + \gamma_{21}q_2 + \gamma_{12}q_1 + \gamma_{14}q_1 = \big(2-\gamma_{11}\big)q_1$.

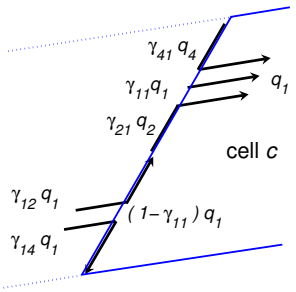

FIGURE 14. Entries from one side in cell c: $(\gamma_{41}q_4+\gamma_{11}q_1+\gamma_{21}q_2)+(\gamma_{12}q_1+\gamma_{14}q_1) = q_1 + \big(1-\gamma_{11}\big)q_1 = \big(2-\gamma_{11}\big)q_1$.

7. **Discrete flow model in a cell.** To create displacements in an elementary cell c, which center is (a,b) and lengths are ϵ_1 and ϵ_2 like in figure 13, we build an equivalent of the one dimension *Fundamental Diagram* of traffic flow.

Equation (26) is a discretized version of equation (28). Equations (29), (30) and (31) have same type of discretized equations. The total number N of vehicles in the cell is split into $(N_i)_{i\in\{1,2,3,4\}}$. To create displacements with supply and demand, the relevant quantities are not exactly the numbers N_i but the densities of vehicles per lane: for a given direction i and a given number of vehicles N_i, if there are lots of lanes to direction i, the vehicles density on each lane i will be low; if there are only few of lanes to direction i, density on direction i will be high. The number of vehicles per lane to direction i is $\frac{N_i}{\lambda_i \epsilon_{i+1} \sin\theta}$. (Obviously, if $i=4$, $i+1$ is set equal to 1.) Hence, the density of vehicles travelling to direction i is $\frac{N_i}{\lambda_i \epsilon_1 \epsilon_2 \sin\theta}$ or $\frac{\rho_i}{\lambda_i}$.

In cell c, the discretized model for direction 1 is:

$$\begin{aligned}
&N_1(t+\Delta t) - N_1(t) = \\
&\quad f_1(a-\frac{\epsilon_1}{2}, b, t)\epsilon_2 \sin\theta \Delta t \\
&\quad - f_1(a+\frac{\epsilon_1}{2}, b, t)\epsilon_2 \sin\theta \Delta t \\
&\quad + \gamma_{21}(a, b-\frac{\epsilon_2}{2}) f_2(a, b-\frac{\epsilon_2}{2}, t)\epsilon_1 \sin\theta \Delta t \\
&\quad - \gamma_{14}(a, b-\frac{\epsilon_2}{2}) f_1(a, b-\frac{\epsilon_2}{2}, t)\frac{\lambda_2(a, b-\frac{\epsilon_2}{2})}{\lambda_1(a, b-\frac{\epsilon_2}{2})}\epsilon_1 \sin\theta \Delta t \\
&\quad + \gamma_{41}(a, b+\frac{\epsilon_2}{2}) f_4(a, b+\frac{\epsilon_2}{2}, t)\epsilon_1 \sin\theta \Delta t \\
&\quad - \gamma_{12}(a, b+\frac{\epsilon_2}{2}) f_1(a, b+\frac{\epsilon_2}{2}, t)\frac{\lambda_2(a, b+\frac{\epsilon_2}{2})}{\lambda_1(a, b+\frac{\epsilon_2}{2})}\epsilon_1 \sin\theta \Delta t. \qquad (34)
\end{aligned}$$

8. **Fundamental relation in a cell.** The traffic flows in a cell will be determined with a min-*formula*, following the idea of equation (4). Why not use a Macroscopic Fundamental Diagram (see [6, 4])? Because while aggregating the data as the MFD do, the network geometry is lost: it is as if the network were isotropic. In this section, we want to construct supply and demand functions in a traffic cell in order to keep the network anisotropy and take the intersection conflicts into account.

8.1. **Network supply in a cell.** The definition of the network supply in a given cell c is a very tough task.

8.1.1. *Cell capacity.* The cell capacity K_c could be defined as the capacity of any lane in the cell. Hence, we suppose that all lanes have nearly the same capacity. This definition is only theorical. As vehicles are spread in a cell, conflicts imply that capacity should never be reached. But it will help to define the cell supply.

8.1.2. *Cell supplies.* We want to define the cell supply for each direction i. Let us consider $i = 1$. The supply for vehicles which want to enter cell c with direction 1 is a function of the lanes densities $(\frac{\rho_1}{\lambda_1}, \frac{\rho_2}{\lambda_2}, \frac{\rho_4}{\lambda_4})$.

We build the supply function as a product: $S_1 = \lambda_1 K_c \xi_1(\frac{\rho_1}{\lambda_1})\xi_2(\frac{\rho_2}{\lambda_2})\xi_4(\frac{\rho_4}{\lambda_4})$. We generalize this formula for all i:

$$\forall i,\ S_i = \lambda_i K_c \Pi^4_{j=1,j\neq i+2} \xi_j(\frac{\rho_j}{\lambda_j}). \tag{35}$$

For any lane to direction i, function ξ_i is not a supply function, it does not have any dimension. We suppose the capacity drop to be immediate because turning movement rates imply immediately that vehicles are spread in the cell, creating conflicts and decreasing the supply. Hence, ξ functions have no constant part like in figure 1.c. Figure 15 gives a possible function ξ_i, with $r_i^{\max} = \frac{\rho_{i\ \max}}{\lambda_i}$. As soon as one direction is completely blocked, vehicles in other directions cannot cross intersections, hence all vehicles in cell c are blocked.

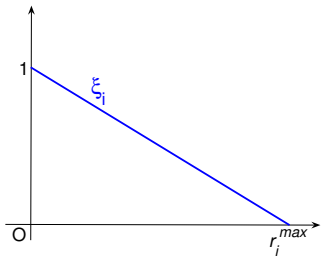

FIGURE 15. Graph of a function ξ in cell c. It is not a supply function, as it does not have any dimension. It traduces the decrease of supply in a given direction i: the presence of vehicles to direction i implies the presence of vehicles to the other directions thanks to turning movement rates.

8.2. **Users' demand in a cell.** On each lane to direction i, let us consider the demand function δ_i. This function is supposed to be the same for each lane to direction i in the cell, it is of classical shape (figure 16). We build the demand function in cell c as:

$$D_i = \lambda_i \delta_i\Big(\frac{\rho_i}{\lambda_i}\Big). \tag{36}$$

Contrarily to supply function, users' demand to direction i while entering in a cell is not a function of the four densities. As there are no internal exchange per direction in each cell, vehicles which want to enter a cell with direction i can already be supposed with direction i.

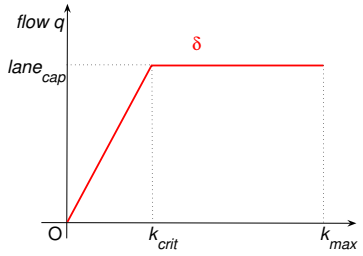

FIGURE 16. Demand function on a lane of cell c. The number lane_{cap} is the lane capacity, k_{crit} is the critical density on the lane and $k_{\max}$ is the maximum density on the lane.

8.3. **Traffic flows generation.** The flow entering in cell c with direction i from cell c_i^- is $f_i = \min(D_i^-, S_i)$, where D_i^- is the partial demand in cell c_i^-. The flow exiting out of cell c with direction i to cell c_i^+ is $f_i = \min(D_i, S_i^+)$, where S_i^+ is the partial supply in cell c_i^+. Figure 17 summarize it for entering flows in a cell (given that an entering flow in a cell is an exiting flow from an adjacent cell).

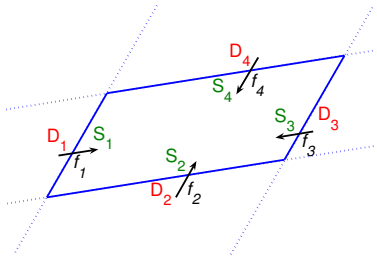

FIGURE 17. Entering flows in a cell viewed with supply and demand.

8.4. **Algorithm.** To build the final algorithm, the inputs are the number of vehicles on each direction and in each cell of the area; the supplies and demands at time $t = 0$ on the whole area (more precisely on every cell of the area); the supply and demand at every time on the border of the area. For instance, it is easy to begin with an empty network. The outputs are the traffic flows and the densities.

Algorithm 2 Large anisotropic continuous network algorithm

Input: density functions λ_i
turning movement rate functions γ_{ij}
border conditions: supplies S_i and demands D_i at the network entries and exits
ending time T

1: empty network initial conditions (at $t = 0$): ρ_i^0 is null
2: **for** $t = 0$ to T **do**
3: Calculate S_i^t and D_i^t with the Supply and Demand functions (35) and (36)
4: Calculate f_i^t with the min-*formula*
5: Calculate ρ_i^{t+1} with the discretized formulas of type (34)
6: **end for**
7: **Output:** the flows f^t, $t = 0 \dots T$, the densities ρ^t, $t = 0 \dots T$.

9. **Conclusion.** We have established a set of dynamical equations that describe the traffic flows and their conflicts in an elementary cell of an anisotropic continuous network. Another idea is to apply homogenization theory on such networks as in [1]; in this article, the intersection conflicts are not modelled, it is just highlighted that an extra virtual link, where vehicles can waste time, can replace the intersection.

10. **Appendix: Stochastic matrices.** Here are some simple results with respect to stochastic matrices.

The matrix $A = (a_{ij}) \in \mathcal{M}_n(\mathbb{R})$ is said to be stochastic if:

$$\begin{cases} \forall (i,j) \in \{1,\dots,n\}^2, & 0 \leqslant a_{ij} \leqslant 1, \\ \forall i \in \{1,\dots,n\}, & \sum_{j=1}^n a_{ij} = 1. \end{cases}$$

It is easy to prove that if λ is an eigenvalue of A, then $|\lambda| \leqslant 1$. A admits the eigenvalue 1 with associated eigenvector ${}^t(1,\dots,1)$. As the characteristic polynomials of matrices A and ${}^tA$ are equal, matrix ${}^tA$ admits 1 as an eigenvalue (but we don't know a priori an eigenvector). We are going to prove a very simple result (we did not see it in any exercise book):

Lemma 10.1. *An eigenvector of ${}^tA$ associated to the eigenvalue 1 can be chosen with all its coordinates positive or null.*

Proof. Let us take an eigenvector $X = (x_i)$ of ${}^tA$ with associated eigenvalue 1. As matrix ${}^tA$ is a real matrix and 1 is a real eigenvalue of ${}^tA$, X can be chosen as a real vector. We are going to prove that $Y = (|x_i|)$ is an eigenvector ${}^tA$ with associated eigenvalue 1.

Let us denote N, Z and P the three sets that define a partition of $\{1,\dots,n\}$:

$$\begin{aligned} N &= \{i \in \{1,\dots,n\} / \, x_i < 0\}, \\ Z &= \{i \in \{1,\dots,n\} / \, x_i = 0\}, \\ P &= \{i \in \{1,\dots,n\} / \, x_i > 0\}. \end{aligned}$$

$$\begin{aligned}\forall i,\, x_i &= \sum_{k=1}^{n} a_{ki}x_k \\ &= \sum_{k\in N} a_{ki}x_k + \sum_{k\in Z} a_{ki}x_k + \sum_{k\in P} a_{ki}x_k\end{aligned}$$

Then $\forall i \in N$, $x_i \geqslant \sum_{k\in N}^{n} a_{ki}x_k$. Then $\sum_{i\in N}^{n} x_i \geqslant \sum_{i\in N}^{n}\sum_{k\in N}^{n} a_{ki}x_k$ then $\sum_{i\in N}^{n} x_i \geqslant \sum_{k\in N}^{n} x_k \sum_{i\in N}^{n} a_{ki}$ which is equivalent to $\sum_{i\in N}^{n} x_i \geqslant \sum_{i\in N}^{n} x_i \sum_{k\in N}^{n} a_{ik}$ $\sum_{i\in N}^{n} x_i\big(1 - \sum_{k\in N}^{n} a_{ik}\big) \geqslant 0$

As $x_i < 0 \forall i \in N$, we obtain that $\forall i \in N$, $1 - \sum_{k\in N}^{n} a_{ik} = 0$. We can conclude that $\forall i \in N$, $(j \in Z \cup P) \Rightarrow a_{ij} = 0$. Hence, $\forall i \in N$, $\sum_{k\in Z\cup P}^{n} a_{ki}x_k = 0$.

For all $i \in N$:

$$\begin{aligned}\sum_{k=1}^{n} a_{ki}|x_k| &= \sum_{k\in N} a_{ki}(-x_k) + \sum_{k\in Z\cup P} a_{ki}x_k \\ &= -\sum_{k\in N} a_{ki}x_k - \sum_{k\in Z\cup P}^{n} a_{ki}x_k \\ &= -\sum_{k=1}^{n} a_{ki}x_k \\ &= -x_i \\ &= |x_i|\end{aligned}$$

By the same token on x_i with $i \in P$, we have $\forall i \in P$, $(j \in N \cup Z) \Rightarrow a_{ij} = 0$. Hence, $\forall i \in P$, $\sum_{k\in N\cup Z}^{n} a_{ki}x_k = 0$. For all $i \in P$, we have $\sum_{k=1}^{n} a_{ki}|x_k| = |x_i|$.

We end by the case $i \in Z$:

$$\begin{aligned}\sum_{k=1}^{n} a_{ki}|x_k| &= \sum_{k\in N} a_{ki}(-x_k) + \sum_{k\in P} a_{ki}x_k \\ &= 0 \\ &= |x_i|\end{aligned}$$

□

Remark 1. We can prove this last result with Brouwer's theorem. Let us consider the convex compact subset of $\mathbb{R}^n$: $C = \{\forall i,\, x_i \geqslant 0,\, \sum_{i=1}^{n} x_i = 1\}$. The map $f : \mathbb{R}^n \to \mathbb{R}^n$ defined by $f(x) =^t A.x$ is continuous and $f(C) \subset C$. Hence there exists (at least) one fixed point of f in C, which proves the result.

REFERENCES

[1] Jean-Bernard Baillon and Guillaume Carlier, *From discrete to continuous Wardrop equilibria*, Networks and Heterogeneous Media, **7** (2012), 219–241.

[2] Giuseppe Maria Coclite and Benedetto Piccoli, "Traffic Flow on a Road Network," Technical Report, SISSA, 2002.

[3] Giuseppe Maria Coclite, Mauro Garavello and Benedetto Piccoli, *Traffic flow on a road network*, SIAM J. Math. Anal., **36** (2005), 1862–1886.

[4] Nikolas Geroliminis and Carlos Daganzo, *Existence of urban-scale macroscopic fundamental diagrams: Some experimental findings*, Transportation Research B, **42** (2008), 759–770.

[5] Helge Holden and Nils Henrik Risebro, *A mathematical model of traffic flow on a network of unidirectional roads*, SIAM J. Math. Anal., **26** (1995), 999–1017.

[6] Yangbeibei Ji, Winnie Daamen, Serge Hoogendoorn, Sascha Hoogendoorn-Lanser and Xiaoyu Qian, *Investigating the shape of the macroscopic fundamental diagram using simulation data*, Transportation Research Record: Journal of the Transportation Research Board, Transportation Research Board of the National Academies, Washington D. C., **2161** (2010), 40–48.

[7] Jean-Patrick Lebacque, *The Godunov scheme and what it means for first order traffic flow models*, Transportation and Traffic Theory. Proceedings of the 13th ISTTT (J. B. Lesort Editor), Elsevier (1996), 647–677.

[8] Jean-Patrick Lebacque and Megan Khoshyaran, *Macroscopic flow models: Intersection modeling, network modeling*, Transportation planning: The state of the art. Kluwer Academic Press, 6th Meeting of the Euro Working Group on Transportation (2002), 119–139.

[9] Jean-Patrick Lebacque and Megan Khoshyaran, *First-order macroscopic traffic flow models: Intersection modeling, network modeling*, Transportation and Traffic Theory. Flow, Dynamics and Human Interaction, 16th International Symposium on Transportation and Traffic Theory (2005), 365–386.

[10] M. H. Lighthill and G. B. Whitham, *On kinematic waves II: A theory of traffic flow on long crowded roads*, Proceedings of the Royal Society, London, **A, 229** (1955), 317–345.
[11] Luis Miguel Romero Prez and Francisco García Benítez, *Traffic flow continuum modeling by hypersingular boundary integral equations*, International Journal for Numerical Methods in Engineering, **82** (2010), 47–63.
[12] Paul I. Richards, *Shock-waves on the highway*, Operations Research, **4** (1956), 42–51.
[13] Azuma Taguchi and Masao Iri, *Continuum approximation to dense networks and its application to the analysis of urban road networks. Applications*, Mathematical Programming Study, **20** (1982), 178–217.
[14] John Glen Wardrop, *Some theorical aspects of road traffic research*, Proceedings of the Institute of Civil Engineers, **II** (1952), 328–378.
[15] S. C. Wong, *Multi-commodity traffic assignement by continuum approximation of network flow with variable demand*, Transportation Research B, **32** (1998), 567–581.
[16] Hai Yang, Sam Yagar and Yasunori Iida, *Traffic assignment in congested discrete/ continuous transportation system*, Transportation Research B, **28** (1994), 161–174.

Received August 2012; revised July 2013.

E-mail address: tibye.saumtally@ifsttar.fr
E-mail address: jean-patrick.lebacque@ifsttar.fr
E-mail address: habib.haj-salem@ifsttar.fr